

ChemComm

Accepted Manuscript



This is an *Accepted Manuscript*, which has been through the Royal Society of Chemistry peer review process and has been accepted for publication.

Accepted Manuscripts are published online shortly after acceptance, before technical editing, formatting and proof reading. Using this free service, authors can make their results available to the community, in citable form, before we publish the edited article. We will replace this *Accepted Manuscript* with the edited and formatted *Advance Article* as soon as it is available.

You can find more information about *Accepted Manuscripts* in the [Information for Authors](#).

Please note that technical editing may introduce minor changes to the text and/or graphics, which may alter content. The journal's standard [Terms & Conditions](#) and the [Ethical guidelines](#) still apply. In no event shall the Royal Society of Chemistry be held responsible for any errors or omissions in this *Accepted Manuscript* or any consequences arising from the use of any information it contains.

COMMUNICATION

Caught! Crystal Trapping of a side-on peroxo bound to Cr(IV)[†]

Cite this: DOI: 10.1039/x0xx00000x

David P. de Sousa,^a Jennifer Bigelow,^b Jonas Sundberg,^a Lawrence Que Jr.,^b and Christine J. McKenzie^{*a}

Received 00th January 2014,
Accepted 00th January 2014

DOI: 10.1039/x0xx00000x

www.rsc.org/

A Cr(IV) η^2 -peroxo complex crystallizes from 33% aqueous H₂O₂. The complex is a likely intermediate in catalytic disproportionation of H₂O₂ proposed to occur through a single metal site mechanism in solution - and solid state.

The study of metal-dioxygen, peroxo and oxo adducts has attracted considerable attention as such metal-activated oxygen species have emerged as the common precursors and active oxidants in a wide range of biological and non-biological oxidation systems.^{1–5} The majority of first row transition metals are represented as co-factors in enzymes and proteins. However, in spite of its rich redox chemistry, reasonable availability and oxophilicity, chromium is by large absent in the natural world. Instead, it is generally considered a cell toxin capable of causing damage to DNA and RNA, through both oxidative mechanisms and adduct formation.^{6,7} Several molecular Cr(V)-oxo complexes have been reported in the literature over the last 40 years,^{8–13} whereas only a handful Cr-peroxo complexes have been identified. In all cases these compounds are derived from the reaction of Cr(II) precursors with O₂. An ion proposed to be a Cr(III)-superoxo complex [CrO₂(bipy)₂]²⁺ (bipy = 2,2'-bipyridine) was obtained by reacting coordinatively unsaturated [Cr(bipy)₂]²⁺ with O₂ in the gas phase.^{14,15} Subsequently Theopold *et al.*¹⁶ structurally characterized a “side-on” Cr(III)-superoxo adduct generated from the reaction of [Cr^{II}(Tp^{tBu,Me})NC₆H₅]⁺ (Tp^{tBu,Me} = hydrotris(3-tert-butyl-5-

University of Minnesota, Minneapolis, Minnesota, 55455, USA

[†] Electronic Supplementary Information (ESI) available: Experimental details of syntheses, crystal structure determination, spectroscopic techniques and supporting CV, EPR, ESI-MS, GC-TCD, rR and time-resolved UV-Vis spectra. CIF files available from the CCDC (1031521 - 1031522). See DOI: 10.1039/c000000x/

methylpyrazolyl)borate) with O₂ in diethylether. Recently Nam *et al.* have reported both an “end-on” Cr(III)-superoxo¹¹ and a “side-on” Cr(IV)-peroxo¹⁷ adduct supported by macrocyclic tetramethylcyclams of different ring sizes.

Molecular Cr-peroxo species are relevant with respect to the biotoxicity of chromium, and are useful as structural mimics of more elusive metal-dioxygen adducts of the later transition metals. We have previously used amino-acid derived pyridine ligands, such as tpena[−] (*N,N,N*-tris(2-pyridylmethyl)ethylenediamine-*N'*-acetate), to generate reactive iron(IV)-oxo,^{18,19} manganese(IV)-oxo complexes and putative O₂ adducts,^{20,21} and a metal-oxidant (iodosylbenzene) adduct.²² The instability of such high-valent iron and manganese complexes makes their structural characterization especially difficult. The isolation of more stable structural analogues based on earlier first row transition metals is a potentially fruitful strategy for glean structural information on such intermediates.¹⁸ Here we describe the structural trapping of a catalytically competent Cr(IV)-peroxo adduct formed from the reaction of a Cr(III) precursor with H₂O₂.

[Cr^{III}(tpena)]²⁺ (**1**) is prepared in aqueous solution from the reaction of chromium(III)-nitrate with the sodium salt of the ligand, followed by crystallization as a diperchlorate salt. The X-ray crystal structure shows that tpena[−] coordinates through all six donor atoms. The Cr(III) atom displays a particularly irregular octahedral geometry, Fig. S1, most notable being an extremely obtuse N1-Cr-N5 angle of 115.40(4)°. When dissolved, UV-Vis spectra (pH 4–8) show that aqueous solutions contain an

^a Department of Physics, Chemistry and Pharmacy, University of Southern Denmark, Campusvej 55, 5230 Odense M (Denmark). Fax: +45 6615 8760; Tel: +45 6550 2518; E-mail: mckenzie@sdu.dk

^b Department of Chemistry and Center for Metals in Biocatalysis,

equilibrium between **1**, its “pseudo hydrate”, $[\text{Cr}^{\text{III}}(\text{tpenaH})\text{OH}]^{2+}$ (**2**) and the blue congener base $[\text{Cr}^{\text{III}}(\text{tpena})\text{OH}]^+$ (**3**), Scheme 1. Complex **3** is the base peak in ESI-MS spectra and this speciation is supported by cyclic voltammetry, *vide infra*. Addition of base drives the equilibrium towards **3**. If 100 eq of H_2O_2 are added to solutions of **1** a colour change from red to violet occurs over 30 mins accompanied by the evolution of dioxygen²³ consistent with modest catalase activity. The solutions are EPR silent.

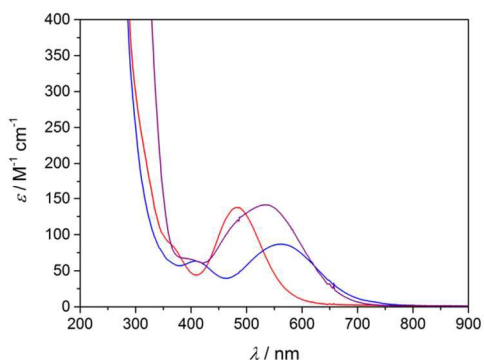


Fig. 1 Aqueous UV-Vis spectra of 4 mM **1** (red line), 3.7 mM **4** (violet line, generated *in-situ* from **1** and 200 eq H_2O_2) and 3.6 mM **3** (blue line, generated *in-situ* from **1** and 50 eq NaOH).

This observation, together with UV-Vis spectroscopy (λ , 539 nm; ϵ , $150 \text{ M}^{-1}\text{cm}^{-1}$), Fig. 1, and electrospray ionization (ESI) mass spectra - which show the dominant presence of a Cr(tpena)-dioxygen adduct $[\text{CrO}_2(\text{tpena})]^+$ at m/z 474.1 (calcd. 474.1), suggests either of the isomeric species: a triplet Cr(III)-superoxo system consisting of a Cr(III) center anti-ferromagnetically coupled to a $\text{O}_2^{\cdot-}$ radical, or a triplet Cr(IV)-peroxo system. A Cr(III)-hydroperoxo adduct was ruled out, since this formulation would give rise to a simple 3/2 system presumably with a spectrum similar to that obtained for **1**, Fig. S5. The presence of a band at 878 cm^{-1} in the resonance Raman spectrum of the purple solutions, Figs. 2(a) and S8(b) (full spectrum) identifies the species unambiguously as a peroxo, rather than a superoxo complex.²⁴ Consistently the IR spectrum of an EPR silent solid precipitated with diethyl ether/dioxane shows a strong sharp absorption at 871 cm^{-1} not seen in IR spectrum of **1**, Fig. 2(b). The differences in the ligand vibrations at 1256, 1373 and 1669 cm^{-1} suggests that a pyridine arm of the ligand is uncoordinated and protonated as seen in the salts of $[\text{V}^{\text{IV}}\text{O}(\text{tpenaH})]^{2+}$ and $[\text{Fe}^{\text{III}}_2\text{O}(\text{tpenaH})_2]^{4+}$,^{18,22} and the formulation $[\text{Cr}^{\text{IV}}\text{O}_2(\text{tpenaH})]^{2+}$ (**4**) could be proposed.

Single crystals of $4(\text{ClO}_4)_2(\text{H}_2\text{O}_2)_3(\text{H}_2\text{O})$ were obtained only on a couple of occasions by placing the largest crystals of $1(\text{ClO}_4)_2(\text{C}_4\text{H}_8\text{O}_2)_{0.5}$ available in aqueous 33% H_2O_2 . Over the course of a day at 4°C the starting material was replaced by plates of the purple peroxo complex. Bubbles of O_2 were observed to slowly emerge from both the solution and the surface of the crystals. The X-ray crystal structure, Fig. 3(a), shows that the peroxide is coordinated to a seven coordinated Cr-centre in a side-on fashion, and charge balance dictates that the cation is a Cr(IV) species. As anticipated one methylpyridyl

arm is uncoordinated and protonated. The distance between the O atoms of the O_2 moiety is $1.383(8) \text{ \AA}$. The average Cr-L distances for **1** and **4** respectively are $2.040(1) \text{ \AA}$ and $2.014(6) \text{ \AA}$ supporting a higher oxidation for the chromium ion in **4**. The +4 oxidation state is confirmed by a Bond Valence Sum (BVS) analysis which yields a $\text{BVS} = 4.001$.²⁵ A hydrogen-bonding motif is present in the crystal, with the cations linked together by the protonated dangling pyridyl arm of one molecule and the non-coordinated carbonyl oxygen of a neighbour ($\text{PyH}^+\cdots\text{OOC}$, 1.904 \AA), forming herringbone chains. The hydrogen-bonded chains stack regularly to form sheets parallel to the *b*-axis, forming the basis for a network of

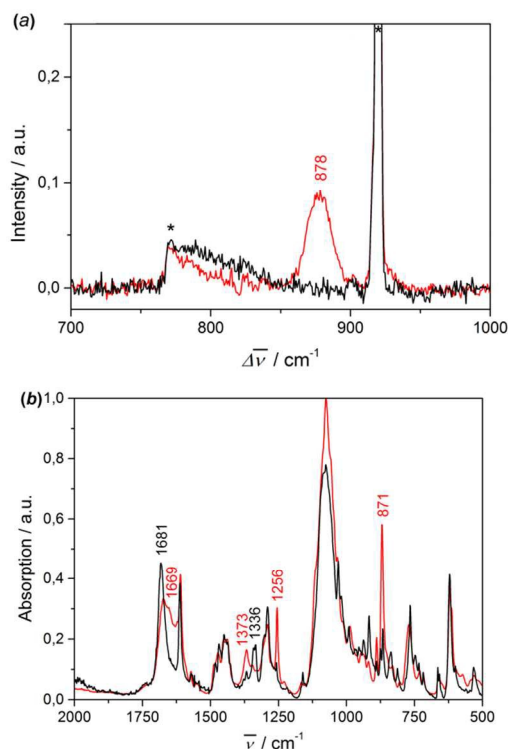


Fig. 2 (a) Frozen solution rRaman spectra of 9 mM **1** (black) and **4** (red) recorded at 77 K in CH_3CN ($\lambda_{\text{ex}} = 514.5 \text{ nm}$, power = 65 mW). Asterisks denote solvent signals. (b) Solid state IR spectra of **1**(ClO_4)₂ (black) and **4**(ClO_4)₂ (red).

pores running along the *c*-axis. The pores are occupied by four co-crystallized H_2O_2 molecules per cation. The perchlorate ions H-bond predominantly to the substrate guest H_2O_2 . The unusually large number of H_2O_2 molecules in the crystal lattice, and their disorder, suggest that these might be rather mobile guests. Thus we conclude that a “crystal trapping” of the reactive **4** is made possible because it is surrounded by substrate which is taken up in the solid state, selectively, from solution. A calculation of the pore dimensions after *in silico* removal of the H_2O_2 molecules reveals about 16% pseudo void space. These voids lie predominantly between internal lamellar surfaces with the coordinated peroxo ligands lining the surface of these sheets, Fig. 3(b). With such a spatial arrangement, it seems reasonable to assume that guest H_2O_2 molecules can creep between the sheets, while product O_2 is able to leave the crystals the same way by diffusion.

Deprotonated **4** (m/z 474.1, $4 - H^+$) is present in ESI mass spectra obtained on both working solutions containing excess H_2O_2 , and in the spectra of isolated $4(ClO_4)_2(H_2O_2)_4$ redissolved in acetonitrile. These spectra furnish some hints about the mechanism of the catalytic H_2O_2 disproportionation, and the decomposition of **4** in the absence of substrate H_2O_2 , respectively. The dominant ion in both spectra is $[Cr^{II}(tpena)]^+$ (**5**; m/z 442.1, calcd. 442.1). While **5** is accessible electrochemically (*vide infra*), it was present, only occasionally, as a minor ion in the spectra of **1** (complex **3** dominates the spectra of **1**, Fig. S2). These observations suggest that **5** is not predominantly formed via an ionization induced one-electron reduction of **1**. Collision Induced Dissociation (CID) experiments on the 474.1 ion ($4 - H^+$) result in the loss of the mass equivalent of two

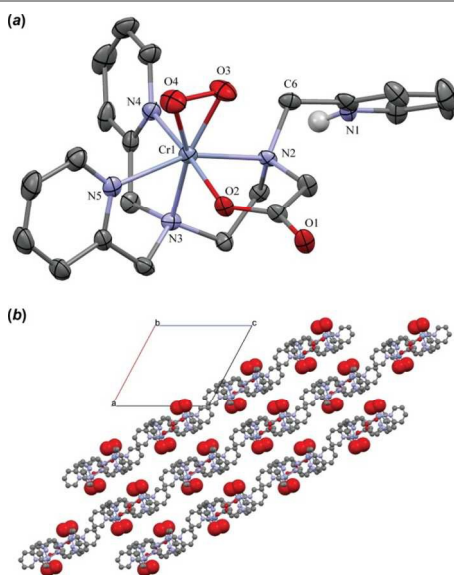


Fig. 3 (a) ORTEP plot of the cation in $4(ClO_4)_2(H_2O_2)_4$ showing 50% probability ellipsoids. (b) Ball-and-stick illustration of the crystal lattice defined by the chains of H-bonded **4** with the peroxide ligand as space filled spheres after *in silico* removal of H_2O_2 and ClO_4^- . Viewed down the b -axis.

oxygen atoms to directly generate **5**. That no stepwise O atom loss occurs, strongly indicates that the O-O bond remains intact during this process¹¹ and that this is the dominant route for generation of the observed Cr(II) species **5**. Ions assigned to $[Cr^{IV}O(tpena)]^+$ (m/z 458.1, calcd. 458.1) and $[Cr^{V}O(tpena)]^{2+}$ (m/z 229.1, calcd. 229.1), and its ion pair, $\{[Cr^{V}O(tpena)]ClO_4\}^+$ (m/z 557.1 calcd. 557.1) and other high-valent O containing species appear only in the spectra of isolated $4(ClO_4)_2$. These species might result from the inter- and intra-molecular O atom transfer from **4** to an unknown substrate or the ligand.²⁸ It is noteworthy that a greater number of ligand decomposition products are observed in Fig 4(b). On the basis of the electronic and geometrical structure of **4**, the gas phase experiments through which various Cr(II), Cr(IV)peroxo, Cr(IV)-oxo, and Cr(V)-oxo species are observed, we propose in Scheme 1, a catalytic acid-base type cycle for the relatively slow disproportionation of H_2O_2 . The cycle is similar to mechanisms proposed for heme catalases.²⁶ Indeed the possible involvement

of a second coordination sphere basic pyridine to aid proton transfers is reminiscent of the role of the proximal histidine in peroxidases. The species labelled by a number have been detected, and a structural analogue for **6**, $[V^{IV}O(tpenaH)]^+$ is known.¹⁸ The direct observation of the O_2 release process step (vi) by CID suggests that the pro-catalyst **1** is not directly involved in the catalytic cycle, but requires reductive activation, by direct (i)+(ii) or

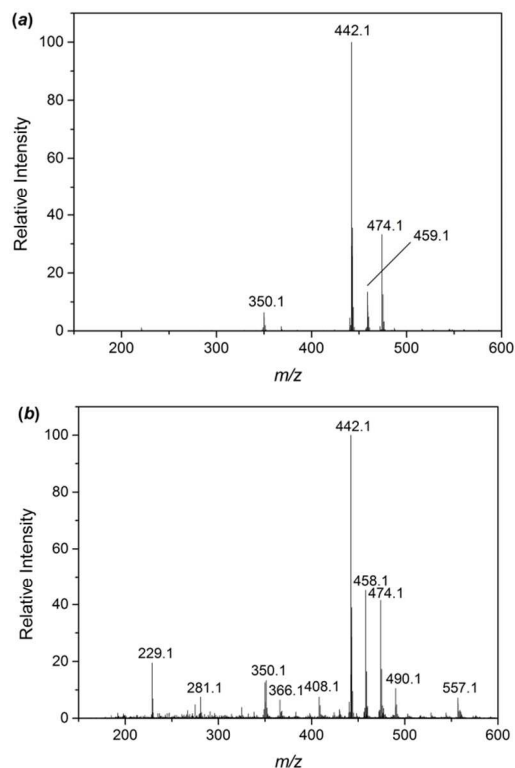
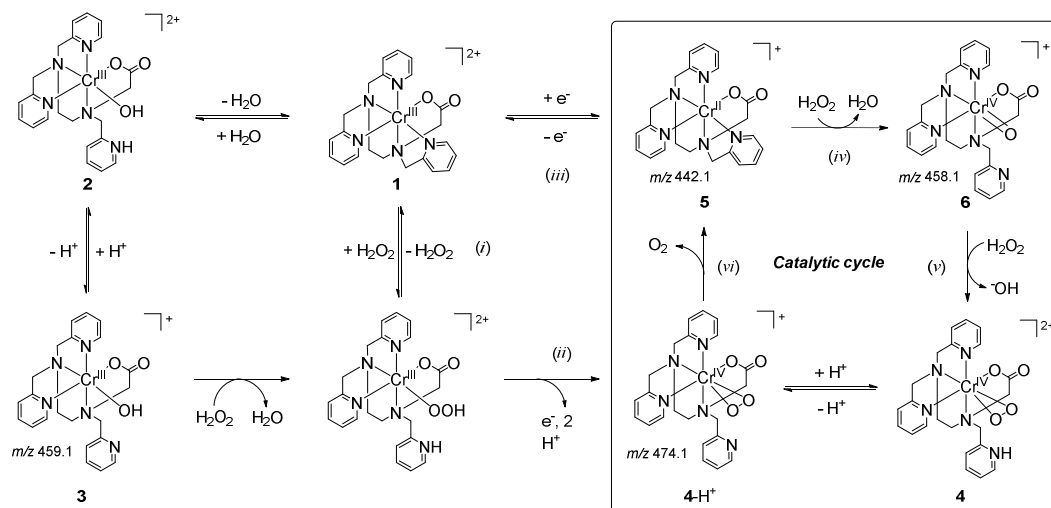


Fig. 4 (a) ESI mass spectrum of solution of **4** generated *in situ* from the reaction of **1** with 200 eq H_2O_2 in H_2O . (b) ESI mass spectrum of $4(ClO_4)_2$ dissolved in CH_3CN . Important assignments not in the text: m/z 490.1 $[Cr^{IV}(O)(O_2)(tpena)]^+$ (or $[Cr^{IV}(O_2)(tpenaO)]^+$), 366.1 $[Cr^{III}(tpenaO-CHC_5H_4N)]^+$, 350.1 $[Cr^{III}(tpena-CH_2C_5H_4N)]^+$.

indirect (iii) involvement by H_2O_2 , before it can enter the cycle. Time-resolved UV-Vis spectroscopy indicates that the direct (i)+(ii) mechanism is the dominant activation pathway, since the time trace for the appearance of the λ_{max} at 553 nm due to the chromophore of **4** can be modelled satisfactorily with a 2-step mechanism (See ESI Fig S7). The cyclic voltammogram of $1(ClO_4)_2$ reveals the presence of **1** and **3** in neutral aqueous solutions, with reversible $Cr^{2+/3+}$ redox couples at $E_{1/2} = -885$ mV and -1099 mV (vs Ag/Ag^+), Fig. S3, supporting the plausibility of the involvement of **5** in the catalytic cycle. The Cr(IV)-oxo species, **6**, formed by a O atom transfer from H_2O_2 to **5** (iv) is expected to be a strong base which can deprotonate H_2O_2 and assist the substitution step (v),²⁵ perhaps with involvement of the dangling pyridine.

In summary, we have isolated a rare example of a side-on Cr(IV)-peroxo adduct. This species is a catalytically competent species in solutions, and within crystals, for catalytic H_2O_2 dismutation. Its preparation involves the reaction of an unusually

labile Cr(III) precursor and H₂O₂. This is an interesting contrast to the syntheses of the handful of other known Cr-O₂ (superoxo, peroxy) adducts which typically involves the reaction of Cr(II) complexes with O₂ - precisely the reverse of step (vi) in Scheme 1.



Scheme 1 Interrelationship between tpena⁺ complexes of Cr(II), Cr(III) and Cr(IV), including a mechanistic proposal for the catalytic decomposition of H₂O₂.

This work was supported by the Danish Council for Independent Research | Natural Sciences (grant 12-124985 to CMcK), and the US National Science Foundation (grant CHE1058248 to LQ). We thank Dr. Mads S. Vad for recording EPR spectra and Simon Svane for performing CID experiments. The COST CM1003 action is acknowledged for travel funding.

Notes and references

- S. J. Lange, L. Que Jr., *Curr. Opin. Chem. Biol.*, 1998, **2**, 159.
- P. C. A. Bruijninx, G. van Koten, R. Gebbink, *Chem. Soc. Rev.*, 2008, **37**, 2716.
- W. A. Van der Donk, C. Krebs, J. M. Bollinger, *Curr. Opin. Struct. Biol.*, 2010, **20**, 673.
- M. Yagi, M. Kaneko, *Chem. Rev.* 2001, **101**, 21.
- R. Huber, P. Hof, R. O. Duarte, J. J. Moura, I. Moura, M. Y. Liu, J. LeGall, R. Hille, M. Archer, M. J. Romão, *Proc. Natl. Acad. Sci.*, 1996, **93**, 8846.
- A. Levina, P. A. Lay, *Chem. Res. Toxicol.* 2008, **21**, 563.
- A. Zhitkovich, *Chem. Res. Toxicol.*, 2005, **18**, 3.
- K. Srinivasan, J. K. Kochi, *Inorg. Chem.*, 1985, **24**, 4671.
- K. H. Nill, F. Wasgestian, A. Pfeil, *Inorg. Chem.*, 1979, **18**, 564.
- T. J. Collins, C. Sleboznick, E. S. Uffelman, *Inorg. Chem.*, 1990, **29**, 3433.
- J. Cho, J. Woo, J. E. Han, M. Kubo, T. Ogura, W. Nam. *Chem. Sci.*, 2011, **2**, 2057.
- M. E. O'Reilly, T. J. Del Castillo, J. M. Falkowski, V. Ramachandran, M. Pati, M. C. Correia, K. A. Abboud, N. S. Dalal, D. E. Richardson and A. S. Veige, *J. Am. Chem. Soc.*, 2011, **133**, 13661–13673.
- S. Liu, K. Mase, C. Bougher, S. D. Hicks, M. M. Abu-Omar and S. Fukuzumi, *Inorg. Chem.*, 2014, **53**, 7780–7788.
- H. Molina-Svendsen, G. Bojesen, C. J. McKenzie, *Inorg. Chem.* 1998, **37**, 1981.
- P. R. Howe, J. E. McGrady, C. J. McKenzie, *Inorg. Chem.*, 2002, **41**, 2026.
- K. Qin, C. D. Incarvito, A. L. Rheingold, K. H. Theopold, *Angew. Chem. Int. Ed.*, 2002, **41**, 2333.
- A. Yokoyama, J. E. Han, J. Cho, M. Kubo, T. Ogura, M. A. Siegler, K. D. Karlin, W. Nam, *J. Am. Chem. Soc.*, 2012, **134**, 15269.
- M. S. Vad, A. Lennartson, A. Nielsen, J. Harmer, J. E. McGrady, C. Frandsen, S. Morup, C. J. McKenzie, *Chem. Commun.* 2012, **48**, 10880.
- W. A. Donald, C. J. McKenzie, R. A. O'Hair, *J. Angew. Chem. Int. Ed.*, 2011, **50**, 8379.
- C. Baffert, M.-N. Collomb, A. Deronzier, S. Kjærgaard-Knudsen, J.-M. Latour, K. H. Lund, C. J. McKenzie, M. Mortensen, L. P. Nielsen, N. Thorup, N. *Dalton Trans.*, 2003, 1765.
- A. K. Poulsen, A. Rompel, C. J. McKenzie, *Angew. Chem.-Int. Ed.*, 2005, **44**, 6916.
- A. Lennartson, C. J. McKenzie, *Angew. Chem.-Int. Ed.*, 2012, **51**, 6767.
- The gas was identified using gas chromatography. TCD detector.
- For a compilation of stretching vibrations for Cr-O₂ complexes, see Table S1 in the electronic supporting information.
- For details and validity of the BVS analysis, see the electronic supporting information.
- M. Alfonso-Prieto, X. Biarnés, P. Vidossich, C. Rovira, *J. Am. Chem. Soc.*, 2009, **131**, 11751.
- U. G. Nielsen, A. Hazell, J. Skibsted, H. J. Jakobsen, C. J. McKenzie, *CrystEngComm*, 2010, **12**, 2826.
- A. Nielsen, F. B. Larsen, A. D. Bond, C. J. McKenzie, *Angew. Chem., Int. Ed.*, 2006, **45**, 1602.